Journal of Urban and Environmental Engineering, v.13, n.1, p.69-79

ISSN 1982-3932
doi: 10.4090/juee.2019.v13n1.069079

Journal of Urban and Environmental Engineering

www.journal-uee.org

PATTERNS OF ENERGY EXCHANGE FOR TROPICAL URBAN AND RURAL ECOSYSTEMS LOCATED IN BRAZIL CENTRAL

Ivan Julio Apolonio Callejas[1*], Marcelo Sacardi Biudes[2], Nadja Gomes Machado[3], Luciane Cleonice Durante[4] and Francisco de Almeida Lobo[5]

[1, 4]*Department of Architecture and Urbanism, Federal University of Mato Grosso, Brazil*
[2]*Institute of Physics, Federal University of Mato Grosso, Brazil*
[3]*Federal Institute of Mato Grosso, Brazil*
[5]*Faculty of Agronomy and Animal Science, Federal University of Mato Grosso, Brazil*

Received 15 August 2018; received in revised form 17 February 2019; accepted 27 February 2019

Abstract: Seasonality and inter-annual variation of the energy balance of natural surfaces as the effect of conversion from natural to agricultural areas has been the object of much in-depth research in South America. However, none has assessed the effect of conversion from native to an urbanized area. Current research was performed in the city of Cuiabá, in the Cerrado-Pantanal ecotone, state of Mato Grosso, central Brazil, featuring a tropical sub-humid climate (Aw). The paper investigates the pattern of energy fluxes exchanges in the rural and urban sites located in Brazilian savannah ecosystem. The heat stored inside the urban canopy (ΔQs) and within the rural area was obtained by the Objective Hysteresis Model (OHM) and by soil flux meter, respectively. Sensible (H) and latent (LE) heat fluxes were estimated by the Bowen Ratio Energy Balance (BREB). The rural and urban sites had different patterns in the micrometeorology variables: wind speed decreased while air temperature and vapor pressure deficit increased from rural to urban site. The urbanization also modified the energy fluxes partition of urban canopy by increasing ΔQs (12%) and H (60%) and by decreasing LE (29%), with β = 2.0, differentiating what was observed in the rural canopy, where the partition was 1.5%, 29%, 64% and β = 0.45, respectively. The ΔQs, H and LE were in phase with Rn, differing from what has been reported for sites in North America and Europe.

Keywords: Urban climate; turbulent flux densities; Bowen ratio; land cover change.

[*] Correspondence to: Ivan J. A. Callejas, Tel.: +55 65 3313 8774; Fax: +55 65 3313 8774.
E-mail: ivancallejas@ufmt.br

INTRODUCTION

The growing population and its concentration in urban centers have accelerated environmental change, mainly due to changes in land cover and to the introduction of other energy sources. Urbanization triggers several environmental effects, such as low dispersion of atmospheric pollutants, reduction in biodiversity, change in the hydrological cycle, change in energy flows and others. Some these effects are attributed to changes in the energy balance caused by conversion from a natural to an urbanized landscape (Oke 1987; De & Mukherjee, 2014).

Whereas energy balance partition in natural or rural areas depends on soil water availability and on vegetation characteristics (Biudes *et al.*, 2015), energy balance partition in urban areas is due to the thermal traits of urban materials (such as thermal conductivity, heat capacity, etc.), fraction of the vegetation-covered and impermeable surface, and urban structure and morphology (Oke, 1987; Offerle *et al.*, 2006). Some studies on surface energy balance in urban areas have been emphasized the differences between urban and rural areas (Coutts *et al.*, 2007; Wang *et al.*, 2015) but also to understand the spatial variability of surface coverage in cities and between cities (Offerle *et al.*, 2006). The differences of the types of urban and rural land use modify the radiation and energy balance and consequently resulting in variations in local climates (Wang *et al.*, 2015). In the last decades, most urban climate research has focused on North American and European cities, located in the northern hemisphere or in temperate climates. In fact, only 6% of urban climate studies in the 1990s were conducted in tropical areas (Jáuregui, 1996), going on to 20% for the 2000s (Roth, 2007).

Climatology studies are on the increase in Brazil, although local and regional investigations have been mainly conducted in southeastern Brazil, with some incursions in the northeastern and northern regions (Amazon Forest), featuring a great lack of information on the mid-western region (Alvares *et al.*, 2014). Several studies on surface energy balance and its partitioning in Brazil assessed their seasonality and the inter-annual variation on natural surfaces and the effect of the conversion from natural to agricultural surfaces (Biudes *et al.*, 2009; Biudes *et al.*, 2015). Few studies on urban surface energy balance were performed (Callejas *et al.*, 2016) and non-evaluated simultaneously the effect of conversion from a native into an urbanized area. Thus, our study focuses in a city located in the Brazilian Midwest within the Cerrado-Pantanal ecotone, which had a fast urban growth in the last decades, without any urban planning, leading to a progressive deterioration of urban environments, particularly the replacement of Cerrado areas by paving and buildings (Callejas *et al.*, 2011).

Since there are few studies on energy balance in urban areas in the Brazilian Midwest and taking into consideration the location of Cuiabá in the Cerrado-Pantanal ecotone, current paper investigates the pattern of energy fluxes exchanges in the rural and urban sites located in the Brazilian savannah ecosystem. We hypothesize that (1) micrometeorology variables and energy balance will have different pattern, and (2) the seasonality in latent and sensitive heat fluxes will be conducted differently in rural and urban sites.

MATERIALS AND METHODS

Site description

Current study was conducted at two different sites located within the transition area between the Pantanal and the Cerrado (Brazilian Savanna) in the south of the state of Mato Grosso, Brazil (**Fig. 1**). The first site comprised an urban area in Cuiabá (CBA), the capital city of the state of Mato Grosso (15°36'36"S; 56°11'04"W). A micrometeorological station was installed in the eastern section of the city characterized by asphalt paving, concrete sidewalks and few four-to-eight-story buildings made of concrete structures coated with bricks and mortar. The roofs are covered with ceramics/fibrocement tiles. The neighborhood is classified as a mixture of commercial, institutional and residential buildings, Class 3, according to the Urban Climate Zones (UCZ) scheme (Oke, 2006).

The second site consisted of a rural area in a mixed woodland-grassland (locally known as campo sujo), on the Miranda Farm (FMI), approximately 15 km from Cuiabá (15°43'53.66" S; 56°04'18.81" W). Native and non-native grasses and semi-deciduous tree species, such as *Curatella americana L.* and *Diospyros hispida A.DC*, are the predominant vegetation (Vourlitis *et al.*, 2013). The regional climate is a semi-humid tropical climate (Aw, following Köppen´s classification) (Alvares *et al.*, 2014), characterized by a dry (May to September) and a wet (October to April) season, with an annual rainfall of 1372.2 mm and average annual temperature of 26.9°C (Machado *et al.*, 2014).

Micrometeorological measurements

A micrometeorological tower was installed at each site, with a continuous collection of data on solar radiation (Rg), net radiation (Rn), air temperature (Ta), relative humidity (RH) and soil heat flux (ΔQ_S). Sensors, data acquisition and power supply systems were nearly identical at the two sites (**Table 1**). All Micrometeorological data were sampled at 10 second intervals using a datalogger and the 30-minute averages were recorded. All sensors were calibrated previously to the campaign to reduce uncertainties (offset and bias) in the measurements.

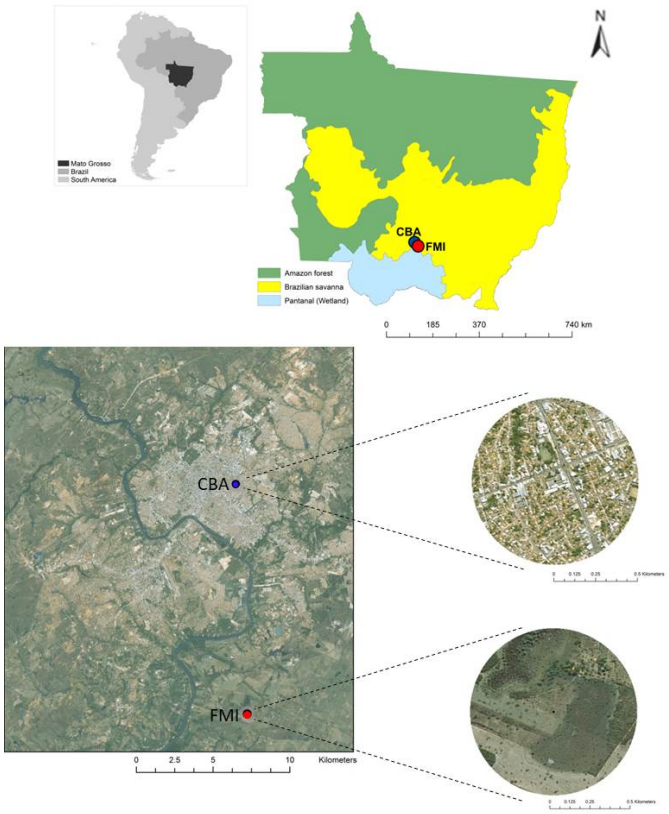

Fig. 1 Location of the urban site in Cuiabá (CBA) and rural site on Miranda Farm (FMI) in the state of Mato Grosso, Brazil

Table 1 Equipment used to measure solar radiation (Rg); net radiation (Rn); air temperature (Ta); relative humidity (RH); soil heat flux (G); and the respective height each sensor was installed at in each experimental area

Sites	Variable	Equipment description	Installed height (m)
FMI	Rg	LI200X, LI-COR, Lincoln, NE, USA	5 m
	Rn	NRLITE, Kipp & Zonen, Delft, Netherlands	5 m
	Ta/RH	HMP-45AC, Vaisala Inc., Woburn, MA, USA	5 m / 18m
	G	HFP01, Hukseflux BV, Delft, The Netherlands	-0,01m
	Data logger	CR 1000, Campbell Sci., Logan, UT, USA	-
CBA	Rg	S-LIB, Onset, Bourne, MA, USA	7.5 m
	Rn	NRLITE, Kipp & Zonen, Delft, Netherlands	7.5 m
	Ta/RH	S-THB, Onset, Bourne, MA, USA	2.5 m / 7.5m
	G	HFP01, Hukseflux BV, Delft, The Netherlands	-0.05 m
	Data logger	U30-NRC, Onset, Bourne, MA, USA	-

Characteristics of land cover and surface

A 500m-radius circle (**Fig. 1**), covering an area of influence of temperature or air humidity sensor, was a footprint in each study site (Oke, 2006). High resolution spatial images were used to describe the sites´ surface characteristics. Plan aspect ratios were retrieved from aerial photographs and a two-dimensional plane area of each type of surface was converted into total area percentage (**Table 2**). Surfaces and their related characteristics were classified into four categories: the plan aspect ratio of building roofs (λ_P); the vegetation plan aspect ratio (λ_V, gardens, lawns, trees, etc); the bare/partially covered soil aspect ratio (λ_S); the plan aspect ratio of impervious surfaces (λ_I) (streets, pavements, car parks, but not buildings). Since walls of buildings contribute towards heat storage in the urban mesh, sophisticated three-dimensional morphometric parameters were utilized in current analysis to estimate the urban heat storage flux inside the urban canopy (ΔQs) by the objective hysteresis model (OHM) (Sun *et al.*, 2017).

Surface energy balance

Surface energy balance of the rural and urban area was calculated by **Eq. (1)**.

$$\mathrm{Rn} + Q_F = \mathrm{H} + \mathrm{LE} + \Delta\mathrm{Q}_s + \Delta\mathrm{Q}_A \qquad (1)$$

where Rn is the net radiation (W m^{-2}); Q_F is the anthropogenic heat flux, neglected in the rural area (W m^{-2}); H is the sensitive heat flux (W m^{-2}); LE is the latent heat flux (W m^{-2}); ΔQ_S is the surface heat storage or soil heat flux (G) (W m^{-2}); ΔQ_A is the net horizontal heat advection (W m^{-2}). Horizontal homogeneity of surface properties and flux densities at ground level were presumed, and the horizontal energy advection was negligible in this work.

In contrast to rural surfaces where soil heat flux was calculated by a soil heat flux plate installed inside the soil, ΔQ_S cannot be measured easily on the urban area. Storage flux on the urban surface is determined by ground (asphalt and concrete) and buildings (roof and wall) which are composed of various materials and orientations. Thus, the urban surface heat flux in CBA was obtained by the parameterization scheme proposed by Grimmond *et al.* (1991). ΔQ_S was calculated as a function of a point source rate of Rn and surface material characteristics were measured by the Objective Hysteresis Model (OHM), according to **Eq. (2)**, which provided a good adjustment with other methods (Roberts *et al.*, 2006).

$$\Delta\mathrm{Q_s} = \sum_1^n(\mathrm{f_i a_{1i}})Rn + \sum_1^n(\mathrm{f_i a_{2i}})\frac{\partial \mathrm{Rn}}{\partial \mathrm{t}} + \sum_1^n(\mathrm{f_i a_{3i}}) \qquad (2)$$

where *i* is one of n surface types of various surface material characteristics fraction (*f*) in the vicinity of CBA, such as roofs, vegetation, soil and impervious paved surfaces, such as concrete and asphalt (see inventory of the local surface cover in **Table 2**).

Table 2 Ratio of three-dimensional (3D) and two-dimensional (2D) area aspect for each category adopted in the vicinity of urban (CBA) and rural (FMI) sites.

Site Information	Location	CBA Site (2D/3D)	FMI Site (2D)
Area Fraction (partial area/total area)	Impervious ratio (λ_I)	28.92% (21.72%)	1%
	Vegetation ratio (λ_V)	15.20% (11.42%)	20.00%
	Soil ratio (λ_S)[1]	10.64% (8%)	78%
	Roof buildings ratio (λ_P)	45.22% (33.97%)	1%
	Urban canyons ratio (λ_C)	0% (24.88%)	-
	Plan area/Tridimensional area[2]	1.33	1.0
Site characteristics	Ground elevation	172m	182m
	Mean building height z_H (m)	6	-
	Land use	Commercial/institutional and residential	Farm
	Roof	Pitched roof (ceramics/ fibro-cement tiles)	-
	Stories	1-2	-
	Walls	Mortar-coated bricks	-
	Vegetation	Deciduous street trees height ≤ building height	Pasture and semi-deciduous tree species
	Surfaces	Asphalt and concrete s	Loamy and silt soil
	Urban Climate Zone (UCZ)[3]	3 (Medium density urban)	7 (Semi-rural)
	Roughness class - z_0 (m)[4]	0.5 (Very rough)	0.1(Roughly open)
	Canyon aspect ratio-ψ_s = H/W	0.5	-0
	Displacement height z_d (m)	2.13	-
	Albedo (α) - Wet (dry)	0.195 (0.191)	0.206 (0.194)

[1]Soil covered by pasture and grass vegetation were included in the partially bare soil; [2]Three-dimensional area was obtained by adding urban canyons areas to plan area; [3]A simplified set of classes that includes aspects of schemes by Ellefsen (1991); [4]Effective terrain roughness according to Davenport classification (Davenport et al. 2000)

Time derivation of net radiation is approximated as $0.5(Rn_{t+1} - Rn_{t-1})$, with t = 1h. The a_{1i}, a_{2i} and a_{3i} are coefficients of each type of *i* surface of CBA environs. The corresponding a_{1i}, a_{2i} and a_{3i} coefficients were derived for the study region utilizing data from CBA (for concrete), FMI (for soil) and Sinop (for vegetation) sites (Callejas *et al.*, 2016). These coefficients were derived monthly to be applied in the model. In the case of roofs and asphalt, data by Meyn & Oke (2009) and Anandakumar (1999) were employed; in the case of urban canyons, data were obtained from Núñez & Oke (1977) and Yoshida et al. (1991) (**Table 3**).

Table 3 Average annual coefficients adopted for OHM Model to estimate the heat flux stored inside the CBA urban canopy.

Surface material	Location/ Author Data	Average annual values a_1 dimensionless	a_2 h	a_3 W m^{-2}
Vegetation	Sinop Forest[1]	0.03	-0.03	-3.3
bare soil	FMI[2]	0.26	-0.07	-22.7
Asphalt	Anandakumar[3]	0.84	-0.83	-19.3
Concrete[4]	CBA	0.21	-0.43	-13.9
Roof	Meyn and Oke	0.07	0.26	-6.0
Urban canyons	Nunez and Oke /Yoshida et al.	0.52	0.03	-34.0

[1]Coefficients determined for Sinop forest located in the Amazon-Cerrado transition zone (Callejas *et al.*, 2016); [2]FMI site soil type is rocky, dystrophic red-yellow Latosol, also known as Plinthosol. [3]Average negative rates of a_2 and a_3 were employed. [4] Coefficients derived monthly from a soil heat flux plate installed under the concrete slab.

Bowen ratio energy balance

Latent (LE) and sensible (H) heat flux were calculated by the Bowen ratio energy balance method (BREB), modified by (Perez *et al.*, 1999) and widely used because of its clear physical concept, few parameter requirements and simple calculation method (Hu *et al.*, 2013). Several researches in the region indicated that BREB method provides accurate and reliable rates and that instrument drifts on sub-annual time scales are minimal (Drexler *et al.*, 2004). LE and H were calculated by **Eq. (3)** and **Eq. (4)**, respectively.

$$LE = \frac{[(Rn+Q_F)-\Delta Q_S]}{1+\beta} \quad (3)$$

$$H = \beta * LE \quad (4)$$

where β is the Bowen ratio is calculate by **Eq. 5**. The anthropogenic heat flux (Q_F) in CBA was estimated by top-down methodology (Sailor & Lu, 2004). The intensity of Q_F rates were small (maximum rate occurred between 7-8AM equal to 11W m^{-2} and minimum between 4-5AM equal to 2W m^{-2}) and negligible in this research (Callejas *et al.*, 2016).

$$\beta = \frac{K_h}{K_e}\left(\frac{c_p}{\lambda\, 0.622}\right)\frac{\Delta T}{\Delta e} \quad (5)$$

where K_h and K_e are the turbulent exchange coefficients for heat and water vapor, c_p is the specific heat capacity at constant pressure (1.00467 J g^{-1} K^{-1}); 0.622 is the ratio of molecular weights of water and air; λ is the latent heat of vaporization (J g^{-1}); ΔT and Δe are differences in temperature (ºC) and water vapor pressure (kPa) between the two measurement levels, respectively. Bowen ratio is based on the assumption that the turbulent exchange coefficients for heat and water vapor are the same ($K_h = K_e$). Thus, we used Bowen ratio regression method (r_{Tq}) proposed by De Bruin *et al.* (1999) as a diagnostic tool to judge whether T-q similarity holds before estimate the fluxes.

The criteria for accepting/rejecting data collected from the BREB method followed Perez *et al.* (1999) and revised by Hu *et al.* (2013). The BREB method fails when (1) sensor resolution is inadequate to solve gradients in ΔT and Δe (Unland *et al.,* 1996); (2) stable atmospheric conditions, especially at dawn and dusk, causing $\beta \sim -1$ (Ortega-Farias *et al.*, 1996), and evapotranspiration tend to infinity; (3) abruptly changing conditions cause errors in the measurement (Perez *et al.*, 1999). Employing the filtering method, physically realistic rates of β may be obtained in a quantitative manner, which limits the potential for bias and error in estimating energy balance terms (Perez *et al.*, 1999; Hu *et al.*, 2013).

Statistical analysis

Gaps in LE and H estimates due to rejection of criteria and/or sensor failure described by De Bruin *et al.* (1999) and Perez et al. (1999) were filled by linear relationships between retained rates of LE and H (dependent variable) and measured rates of $Rn–\Delta Q_S$ (CBA or FMI) (independent variable) (Grace *et al.* 1996). The percentage of available energy (Rn) partitioned into LE and H was determined by linear regression with the origin forced through zero, where daily (24 h) average of LE or H (dependent variables) was regressed against daily Rn over monthly intervals. Regressions´ slope (±95% confidence interval) indicates the relative partitioning of Rn into LE or H. Random errors associated with averages of micrometeorological measurements and energy flux estimates were calculated at ±95% confidence interval over monthly and annual intervals by bootstrapping the resampled time series over 1000 iterations (Efron & Tibshirani, 1993).

RESULTS AND DISCUSSION

Seasonal patterns of meteorological data

Most annual rainfall (97%) occurs between October and April, the region´s wet season (**Fig. 2A** and **Table 4**). The dry season (with total monthly rainfall < 100 mm) lasts 4 months, from May to September. Both sites had a marked increase in rainfall in September, henceforth increasing during each month. The above seasonal trends are consistent with other data retrieved from the region (Biudes *et al.*, 2015; Machado *et al.*, 2014), with a 29% higher increase than normal climatological rates.

There was no significant difference in incident solar radiation (Rg) between the sites and no significant seasonal trend in both sites (**Table 4**). Maximum and minimum Rg averages occur in October and June respectively (**Fig. 2B**). The wet season occurs simultaneously with the period of negative solar declination, or rather, there are high rates of solar radiation at the top of the atmosphere (Rtoa) during the wet season. However, the large amount of cumulus and/or cumulonimbus clouds decrease insolation and consequently the Rg (Li *et al.*, 1995). The highest monthly average of Rg occurred in October due to a high Rtoa and to the small number of clouds, evidenced by low rainfall rates. Low Rg average in June was due to low Rtoa (Machado *et al.*, 2016). The daily Rg seasonal trend was similar for the two sites (Figures 3A and 3B). Maximum rates were higher in the rural area in the two seasons, with differences lower than 4%. The above result fails to agree with several studies on urban climate, demonstrating a greater attenuation of Rg in the urban environment due to greater concentrations of aerosols (Wang *et al.*, 2015).

Although air temperature had no significant seasonal trend (**Table 4**), there was a consistent monthly variation (**Fig. 2C**). Air temperature was significantly correlated with Rg ($r = 0.66$, p-value < 0.001). The lowest monthly mean air temperature occurred in September at the two sites and the lowest average temperature was reported in June in CBA and in May in FMI. Compounded to low Rg rates during the dry season, cold fronts, a common phenomenon between May and July, lowered the region´s air temperature for some days (Machado *et al.*, 2014). The annual air temperature in CBA was 5% higher, whilst air temperature during the wet season in CBA was 6% higher than that in FMI (**Table 2**). However, there was no significant difference in air temperature at the two sites during the dry season. The FMI`s surface, composed of grass and soil, allows the available energy to be primarily used for evapotranspiration (Biudes *et al.*, 2015). Since CBA´s surface is 75% impermeable because of paved streets, sidewalks, parking lots and buildings, the available energy is primarily used for heating the building materials and the air inside the urban canopy (Callejas *et al.*, 2016). On the other hand, although monthly air temperature averages were higher in CBA during the dry season, the sites were not significantly different due to water restriction caused by lack of or low monthly rainfall rates.

Table 4. Total annual and seasonal rainfall, annual and seasonal mean (± 95% Confidence Interval) of solar radiation (Rg; W m-2), air temperature (Ta; ºC), vapor pressure deficit (VPD; kPa), wind speed (m s-1), net radiation (Rn; W m-2), surface heat storage (ΔQs; W m-2), sensible heat flux (H; W m-2), latent heat flux (LE; W m-2) and Bowen ratio (β) in Cuiabá (CBA) and Miranda Farm (FMI) in Mato Grosso State, Brazil.

Variables	CBA			FMI		
	Annual	Wet	Dry	Annual	Wet	Dry
Rainfall	1472.1	1437.2	34.9	1776.2	1712.9	63.3
Rg	196.5±5.4	198.8±9.2	193.4±6.7	197.8±5.8	204.8±7.5	188.0±7.1
Ta	27.9±0.4	28.3±0.3	27.3±0.7	26.6±0.3	26.7±0.3	26.4±0.7
VPD	1.35±0.09	1.06±0.07	1.75±0.15	1.18±0.09	0.87±0.07	1.61±0.15
Ws	0.98±0.03	0.95±0.03	1.02±0.06	1.26±0.06	1.31±0.06	1.20±0.09
Rn	99.1±3.5	102.4±5.5	94.6±4.0	112.8±4.6	128.8±6.0	90.6±5.0
ΔQs	13.1±1.1	13.0±1.7	13.3±1.3	1.7±1.2	-0.1±1.7	4.3±1.6
H	59.0±1.8	60.1±2.7	57.7±1.9	33.1±2.2	35.6±2.9	29.5±3.2
LE	29.1±1.1	31.7±1.5	25.6±1.5	72.3±3.0	85.1±3.7	54.6±3.7
β	2.30±0.12	2.03±0.12	2.65±0.24	0.43±0.05	0.47±0.07	0.37±0.06

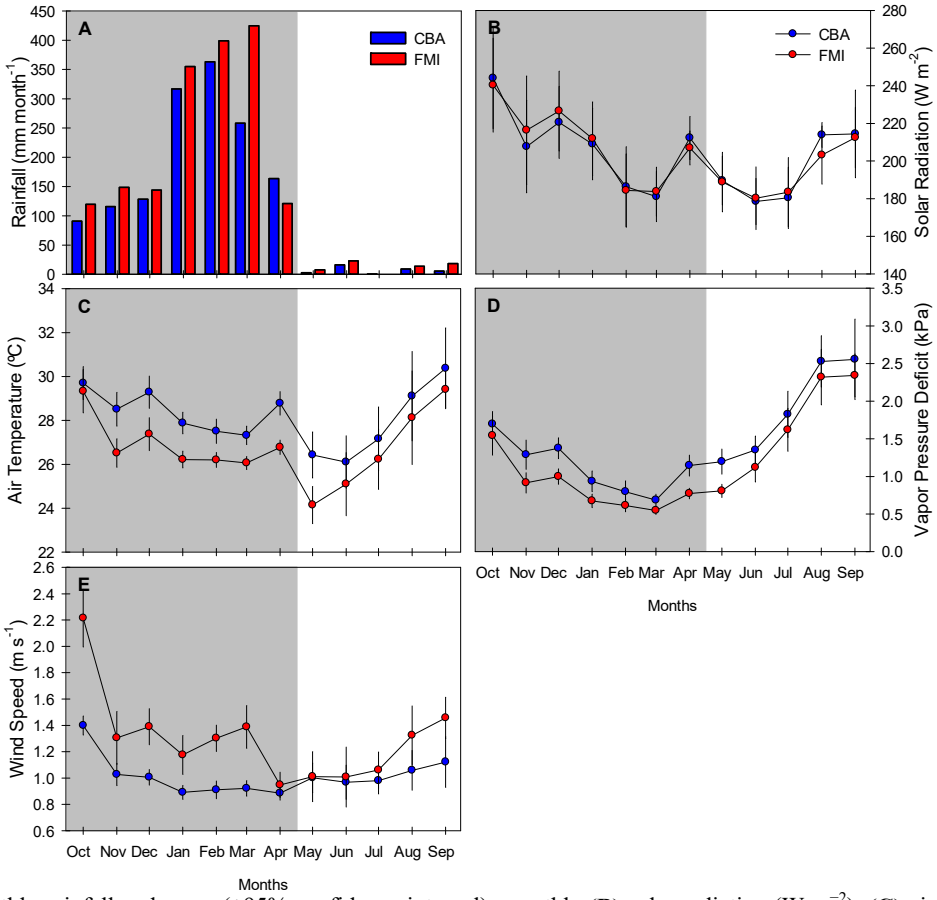

Fig. 2. (A) Total monthly rainfall and mean (±95% confidence interval); monthly **(B)** solar radiation (W m^{-2}); **(C)** air temperature (ºC); **(D)** vapor pressure deficit (VPD, kPa); **(E)** wind speed (m s^{-1}) in Cuiabá (CBA; solid line; black circles) and Miranda Farm (FMI; solid line; white circles). The shaded portion in each figure represents the approximate wet season at the sites under analysis.

Daily air temperature trends were different in CBA and FMI in terms of magnitude and phase (**Fig. 3C** and **Fig. 3D**). The air temperature during the wet season at the two sites had a higher daily average (~1.2ºC), a higher minimum average (~3.2ºC), a lower maximum average (~-0.6ºC) and a lower amplitude average (~-4.0◦C) when compared to that in the dry season. Average minimum air temperatures in CBA were ~0.8ºC higher than those at FMI during the wet and dry seasons. Average maximum air temperature in CBA was 0.9ºC higher and half-hour faster than that in FMI during the wet and dry seasons. The surface in the rural experimental area, with grass and soil, regulates air temperature and humidity inside the rural canopy (Biudes *et al.*, 2015). Thus, the soil energy storage in the rural area is released faster than in the urban canopy.

On the other hand, the surface impermeable areas inside the urban canopy, basically composed of artificial material with low thermal capacity, slowly release energy and maintain air temperature in the urban canopy higher than that in the rural environs, originating the phenomenon of urban heat island (Callejas *et al.*, 2016).

The vapor pressure deficit (VPD) in CBA was 14% higher than in FMI, with a seasonal trend, featuring a 32% higher average in the dry season than in the wet season average (**Table 4**). VPD was inversely correlated with rainfall (r = -0.69; p-value < 0.001), with maximum and minimum averages respectively in September and March (**Fig. 2D**). Since monthly VPD average in CBA was higher than in FMI throughout the year, the urban canopy was drier than the rural one. In fact, FMI surface is characterized by pasture and grass which enhances greater water flow through evapotranspiration than in CBA characterized by a high percentage of impermeable surfaces. Daily VPD had a similar pattern at the two sites during the dry and wet seasons (**Fig. 3E** and **Fig. 3F**), or rather, daily VPD average in the dry season was 47% higher than in the wet season and the maximum and minimum daily averages in the dry season were respectively 43% and 14% higher than in the wet season. The CBA urban canopy remained drier than the FMI rural canopy during the wet season, forming Urban Dry Island in the region. Further, VPD at FMI during the dry season declined faster and had lower rates at night (between 1800h and 0900h) than in the CBA.

The annual average wind speed in FMI was 22% higher than in the CBA, with no significant seasonal variation, although averages in the dry season were numerically higher than in the wet season (**Table 4**). The monthly wind speed average in FMI was higher than in CBA during most of the rainy season (between October and March) (**Fig. 2E**) and affected the highest mean wind speed in FMI during the wet season. The wind´s predominant direction, characterized as higher, during the wet season is generally north and northwest. On the other hand, the dry season is characterized by a lower intensity in wind speed, whilst wind direction is south and southeast.

The daily pattern of wind velocity was similar in the two experimental areas (**Fig. 3G** and **Fig. 3H**). The intensity of the wind speed had a pattern similar to that of incident solar radiation, with a peak shortly after noon and with daytime rates higher than nocturnal ones. Since wind speed in rural and urban areas were weak at night (usually less than 1.0 m s^{-1}), it contributed towards the formation of an urban heat island, especially during the dry season in cloudless conditions. The wind´s highest hourly averages were observed in FMI. The urban canopy provided roughness indexes that formed a zone of influence of deeper friction by which wind speed is reduced when compared to that in rural areas at the same height (Oke, 1987).

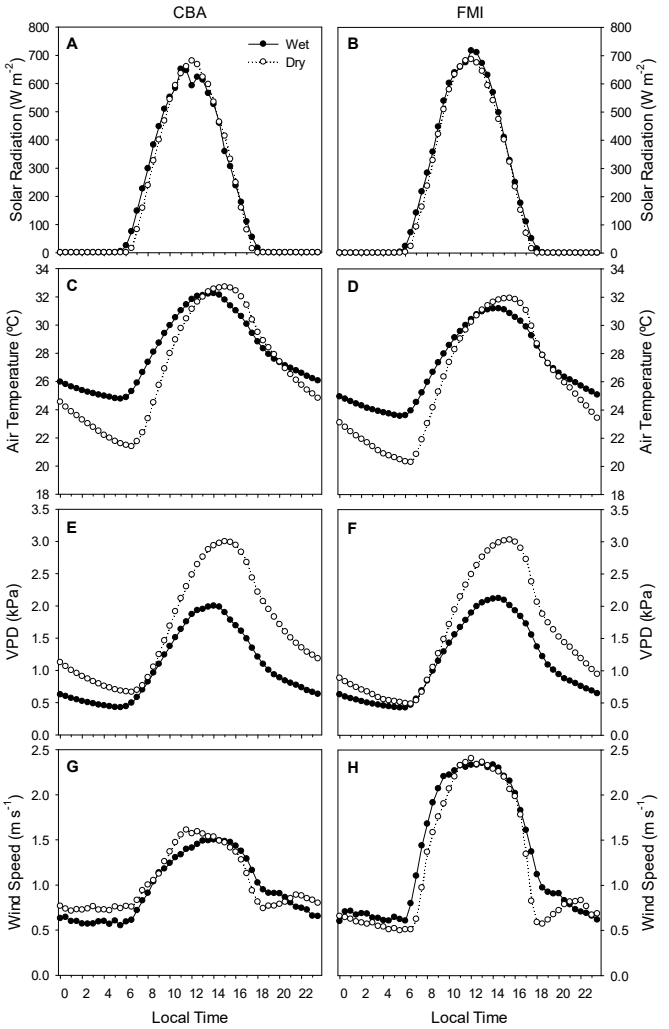

Fig. 3 Seasonal mean hourly **(A)** solar radiation (Rg; W m-2); **(B)** air temperature (ºC); **(C)** vapor pressure deficit (VPD; kPa); **(D)** wind speed (m s^{-1}) at CBA and FMI in the dry and wet seasons. Solid line and black circles represent the wet season, while dotted line and white circles represent the dry season at the sites under analysis.

Seasonal patterns in energy flux

Net radiation (Rn) was positively correlated with Rg in CBA (r =0.59; p-value<0.05) and in FMI (r=0.79; p-value<0.01). Rn´s annual average in FMI was 14% higher than in CBA (**Table 4**). Rn was 42% higher during the wet season in FMI and no significant seasonal variability of Rn in CBA has been reported. Rn´s seasonal variation in FMI, consistent with other investigations undertaken in the region analyzed by current study, may be due to Rg´s seasonality and to variations in the surface albedo as a function of water availability in the soil (Fausto *et al.*, 2014). Rn was positively correlated with monthly rainfall in FMI (r=0.61; p-value<0.05), but not in CBA. The lack of rainfall during the dry season greatly reduces the soil water availability and the albedo. Consequently, vegetation becomes more yellowish in the Cerrado (Fausto *et al.*, 2014; Danelichen *et al.*, 2016). Further, there is a greater biomass burning during the dry season, which releases more aerosols to the atmosphere and decrease the Rg (Li *et al.*, 2006).

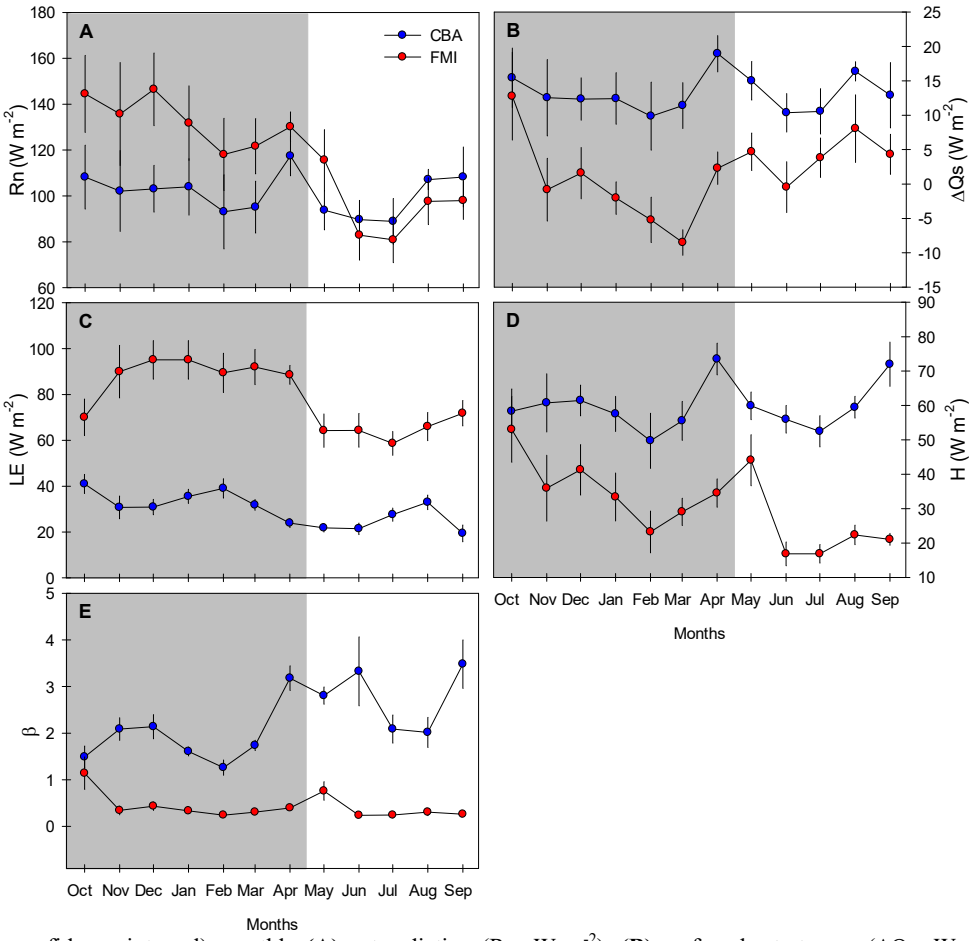

Fig. 4 Mean (±95% confidence interval) monthly **(A)** net radiation (Rn; W m^{-2}); **(B)** surface heat storage (ΔQs; W m^{-2}); **(C)** latent heat flux (LE; W m^{-2}); **(D)** sensible heat flux (H; W m^{-2}) at CBA (solid line; black circles) and FMI (solid line; white circles). The shaded portion in each figure represents the wet season at each site. Note that ΔQs, LE and H heat fluxes are plotted in different scales.

Rn in FMI was 26% higher than in CBA during the rainy season and 4% lower during the dry one. Rn in FMI was higher than in CBA due to a greater effect of air temperature of Rn in CBA (r=0.60; p-value<0.05), while there was no correlation of Rn with the air temperature in the FMI. Rn in CBA did not vary over the months and Rn in FMI was higher than in CBA between October and May and lower between June and September (**Fig. 4A**). The same pattern has been observed in Africa (Offerle *et al.*, 2005) and in Europe (Offerle *et al.*, 2006). The differences in Rn between urban and rural areas were due to thermal and spectrum characteristics of each experimental area influenced by the surface albedo (**Table 2**), radiation geometry of the urban canyon, surface thermal properties and soil water availability (Christen & Vogt, 2004; Coutts *et al.*, 2007). The urban canopy had higher surface temperatures, mainly due to the use of artificial materials which contributed towards a lower availability of water in the soil caused by surface impermeability of the surface within the urban canopy (Callejas *et al.*, 2016). These characteristics modified the radiation balance of the surface of the urban area during the wet season by increasing the long wave radiation emitted by the surface. Consequently, there is a reduction of Rn in the city during daytime. At night, the higher long wave emission and drier atmosphere inside the urban canopy enhance the upwelling long wave radiation. On the other hand, decrease in albedo and water availability at the rural site in the dry season turn its environmental conditions similar to those in the urban site.

Daily Rn patterns at the two sites are similar, with maximum rates at 1200h and negative rates between 1 and 2 hours after sunset (**Fig. 5A** and **Fig. 5B**). It was not possible to identify seasonal differences in the daily Rn pattern in CBA, although Rn during the dry season was lower than in FMI during the wet season. Rn in CBA at night had higher rates (negative) than in FMI. Daily Rn pattern at the two sites was due to daytime Rg pattern, whilst it was due to the heat stored inside the urban canopy and ground (soil) during night time. The seasonal difference observed at both sites may be attributed to the differences in the surface area under analysis. Lower modifications in the surface albedo and higher surface temperature and heat stored inside the urban canopy influenced the lack of seasonality in the daily Rn pattern in CBA and higher negative rates in the night period. Rn patterns were similar in behavior and magnitude to those reported in Miami with similar climate classification (Newton *et al.*, 2007).

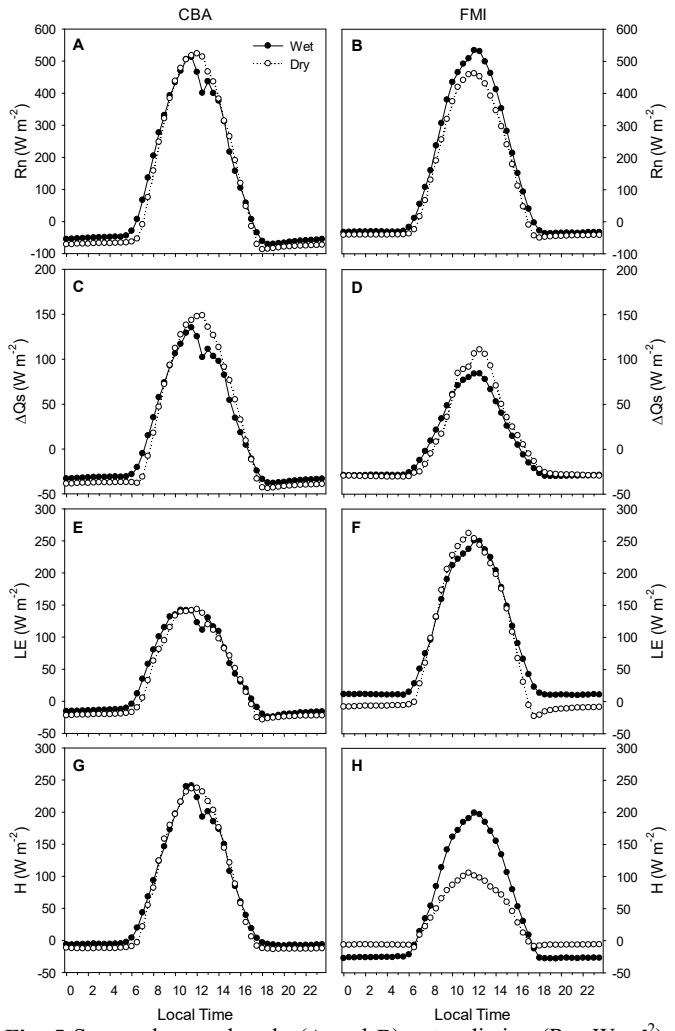

Fig. 5 Seasonal mean hourly (**A** and **B**) net radiation (Rn; W m^{-2}); (**C** and **D**) surface heat storage (ΔQs; W m^{-2}); (**E** and **F**) latent heat flux (LE; W m^{-2}); (**G** and **H**) sensible heat flux (H; W m^{-2}) at CBA and FMI sites. Solid line and black circles represent the wet season, while dotted line and white circles represent the dry season at the sites under analysis.

Annual surface heat storage (ΔQs) average in CBA was 6.7 times greater than that in FMI (**Table 4**). The monthly average was also high throughout the experiment (**Fig. 4B**). There was no seasonal variation of ΔQs in CBA, but ΔQs were significantly higher during the dry season in FMI. The highest ΔQs in CBA were due to the difference in thermal properties of urban fabrics which are different from soils and vegetation surfaces in the rural sites (Christen & Vogt, 2004). In addition, CBA has a larger three-dimensional area (~33%, Table 2) and impervious surfaces within the urban canopy, especially those converted into asphalt paving, concrete and building materials (~ 75% of plan area), which increase the heat stored inside the urban canopy. In fact, ΔQs represented 13% of Rn in CBA, within the range registered for Miami (Newton et al., 2007) and European cities (ranging from 5 to 16%) (Offerle *et al.*, 2006). ΔQs in FMI averaged 1.5% of Rn, ranging between -0.1% during the wet season and 4.7% during the dry season. Unlike the urban canopy, mainly influenced by thermal properties of the constructed material, the seasonality of ΔQs/Rn in FMI was affected by variations in the soil thermal properties and the vegetation cover due to the seasonality of the soil water availability. Results are consistent with previous studies in the region (Biudes *et al.*, 2015, Machado *et al.*, 2016).

The daily pattern of ΔQs (**Fig. 5C** and **Fig. 5D**), in phase with the daily Rn course, with maximum value at 12:00h at the two experimental areas, differs from that reported for the urban canopy in Miami, Florida, where ΔQs intensities were lower than those observed in daytime/nighttime and maximum values peaked 1 to 2 h prior to Rn maximum rate (Newton *et al.*, 2007). Further, ΔQs in CBA was higher during the diurnal and nocturnal period than at FMI and revealed that the urban canopy absorbed more energy during the diurnal period and released slightly more energy during night time when compared to the rural canopy. This is mainly due to the surface´s thermal characteristics, with no three-dimensional surface area and no impervious surfaces, and great seasonal fluctuation rates in the heat store inside the soil because seasonal variations in soil thermal properties affected by variations in rainfall, soil moisture and vegetation coverage.

The Rn was used primarily by the sensible heat flux (H; 60%) in CBA and by the latent heat flux (LE; 64%) in FMI (**Table 4**). The H in CBA was 78% higher than in FMI (**Fig. 4D**) and the LE in FMI was more than twice as large as at CBA (**Fig. 4C**). Sensible heat flux in CBA remained higher than in FMI throughout the period. The reduced LE at the urban site is counterbalanced by increased magnitudes of H and ΔQS (72% of Rn). The pattern of LE and H in the urban area may be attributed to the high impervious surface (~75%) and to low rate in vegetation cover (~15%), which restricts soil water absorption and reduces evapotranspiration. An opposite pattern was observed in the rural area. There was no significant seasonal variation of H in the two experimental areas, but the LE was slightly higher during the wet season in CBA and 56% higher in FMI. Rn percentage in H (60%) and LE (29%) in CBA and FMI (H: 29% and LE: 64%) were similar to those observed in the urban and rural canopy in Switzerland and Poland (Christen & Vogt, 2004; Offerle *et al.*, 2006), and in a previous study at FMI (Rodrigues *et al.*, 2014; Biudes *et al.*, 2015).

The difference in the energy flux patterns of the two sites is due to the complex interaction of radiation with the surface, provided by H and LE correlations with micrometeorological variables. H correlated with air temperature ($r=0.56$; p-value<0.05) and ΔQs ($r=0.73$; p-value<0.01) in CBA, and H correlated with Rg ($r=0.68$; p-value<0.05) and Rn ($r=0.81$; p-value<0.01) in FMI. Thus, H in the urban canopy is conducted primarily by the surface and air temperature inside the urban fabric (Oke, 1987), whereas H in the rural canopy is driven primarily by the amount of solar radiation (Rodrigues *et*

al., 2014; Biudes *et al.*, 2015).

Unlike H, LE correlated with rainfall (r=0.87; p-value<0.001), VPD (r=-0.57; p-value<0.05), Rn (r=0.73; p-value<0.01) and ΔQs (r=-0.65; p-value<0.05) in FMI, but LE wasn't correlated with any micrometeorological variable in CBA. Therefore, LE in the rural canopy is driven by the amount of available energy (Rg and Rn) and the amount of soil and air water availability, indirectly related to the rainfall and VPD, respectively (Rodrigues *et al.*, 2014; Biudes *et al.*, 2015). It was not possible to identify which variable had the greatest influence on LE in the urban canopy due to the complex surface structure of the experimental area.

The Bowen ratio (β) in CBA was 5.4 times higher than in FMI (**Table 4**). There was a seasonal trend in β only in CBA where β during the dry season was 30% higher than during the wet season. It was expected due to higher H in CBA´s artificial materials. As LE is a function of the availability of water on the surface, the elevation of LE in the wet season reduced β rates. Thus, higher β rates were registered at the end of the dry season and at the beginning of the wet one (September and October) and the lowest rates of β in the middle of the wet season (February) (**Fig. 4E**). Bowen ratios were similar to those obtained in urban (β = 1.81-2.47) and rural (β = 0.41-0.55) areas (Christen & Vogt, 2004; Offerle *et al.*, 2006).

LE and H were in phase with Rn, with maximum values during noon at the two experimental areas (**Fig. 5E** and **Fig. 5H**), unlike other studies in North America and Europe, where LE is delayed between 1 and 2 h from Rn. Although the daily patterns of H and LE in CBA and LE in FMI were similar during the dry and humid season, daily rates of H in FMI were higher during the wet season and demonstrates the effect of higher Rn during this period. Maximum daily rates of H and LE were similar to those reported for the urban canopy in North American cities (Grimmond & Oke, 1999; Newton *et al.*, 2007) and for the Cerrado canopy (Biudes *et al.*, 2009; Rodrigues *et al.*, 2014).

CONCLUSION

Simultaneous micrometeorological variables and surface energy balances were estimated in an urban and rural area in Cuiabá in Central Brazil (Köppen climate classification Aw) and permitted to quantify the seasonal patterns of these variables inside the researched sites. We noticed that the interaction between properties of artificial surfaces (building, paving, wall etc), soil and atmosphere inside the urban site combined to produce a different partition on energy balance in relation to those observed in the surrounding rural site.

We confirmed the hypothesis that micrometeorology variables and energy balance will present different seasonal pattern in the researched sites, with latent and sensible heat fluxes being driven differently in rural and urban sites. We found that rural-urban conversion modified micrometeorology variables by decreasing wind speed and by increasing air temperature and the vapor pressure deficit, keeping air temperature and air humidity inside the urban canopy, respectively, higher and lower than the rural canopy.

The modification on the urban energy balance explains why the atmosphere in the urban area has been kept warmer and less moist than its neighboring rural area. The conversion of the savanna into an urban area reduced drastically the vegetation and permeable areas which were converted into asphalt/concrete paving and building materials. Consequently, the energy balance pattern of the urban canopy was modified by increasing ΔQs and H and decreasing LE.

LE was coupled with radiation and water availability in the canopy and H with solar radiation in rural site, while in urban site, H was coupled with surface and air temperature and LE did not have any correlation with any variable. The above demonstrates the complexity of the urban environment, since form, orientation, heterogeneity and fragmentation of urban land contribute towards the production of a particular urban climate. Further research on tropical climate cities in the southern hemisphere must be conducted for more in-depth investigation.

Acknowledgment Current research was partially funded by Conselho Nacional de Desenvolvimento Científico e Tecnológico (MCT-CNPq-CT Infra-CT Energia n. 07/2006; Code: 620082/2006-2; Edital Universal 01/2016, code 407463/2016-0), Fundação de Amparo à Pesquisa do Estado de Mato Grosso - FAPEMAT (Edital Nº 004/2009, code 445139/2009; Edital PRONEM 2014, code 561397/2014). The authors thank the CNPq for concession of the productivity scholarships number 303625/2015-5 and number 310879/2017-5.

REFERENCES

Alvares C.A., Stape J.L., Sentelhas P.C., Golçalves J.L., Sparovek G. (2014) Köppen's climate classification map for Brazil. *Meteorologische Zeitschrift* **22**, 711-718, doi: 10.1127/0941-2948/2013/0507.

Anandakumar K. (1999) A study on the partition of net radiation into heat fluxes on a dry asphalt surface. *Atmos Environ* **33**, 3911-3918, doi: 10.1016/S1352-2310(99)00133-8.

Biudes M.S., Campelo Júnior J.H., Nogueira J.S., Sanches L. (2009) Estimativa do balanço de energia em cambarazal e pastagem no norte do Pantanal pelo método da razão de Bowen. *Rev Bras Meteorol* **24**(2), 135-143, doi: 10.1590/S0102-77862009000200003.

Biudes M.S., Vourlitis G.L., Machado N.G., Arruda P.H.Z., Neves G.A.R.., Lobo F.A., Neale C.M.U., Nogueira J.S. (2015) Patterns of energy exchange for tropical ecosystems across a climate gradient in Mato Grosso, *Brazil. Agric For Meteorol* **202**, 112-124, doi: 10.1016/j.agrformet.2014.12.008.

De Bruin H.A.R., Van Den Hurk B.J.J.M., Kroon L.J.M. (1999) On

the temperature-humidity correlation and similarity. *Boundary-Layer Meteorology* **93**, 453–468.

Callejas I.J.A., Oliveira A.S., Santos F.M.M., Durante L.C., Nogueira M.C.J.A., Zeilhofer P. (2011) Relationship between land use/cover and surface temperatures in the urban agglomeration of Cuiabá/Várzea Grande, central Brazil. *J Appl Remote Sens* **5**(1), 053569, doi: 10.1117/1.3666044.

Callejas I.J.A., Nogueira M.C.J.A., Biudes M.S., Durante L.C. (2016) Seasonal variation of surface energy balance of a central Brazil city. *Mercartor* **15**, 85-106.

Christen A. & Vogt R. (2004) Energy and radiation balance of a central European city. *Int J Climatol* **24**(11), 1395-1421. doi: 10.1002/joc.1074.

Coutts A., Beringer J., Tapper, N.J. (2007) Impact of Increasing Urban Density on Local Climate: Spatial and Temporal Variations in the Surface Energy Balance in Melbourne, Australia. *J Appl Meteor Climatol* 46, 477-493, doi: 10.1175/JAM2462.1.

Danelichen V.H.M, Biudes M.S., Souza M.C., Machado N.G., Nogueira J.S. (2016) Relations of vegetation and water indices o volumetric soil water content in the Pantanal of Mato Grosso, Brazil, *International Journal of Remote Sensing* **37**(18), 4261-4275, doi: 10.1080/01431161.2016.1213921.

Davenport A.G., Grimmond C.S.B., Oke T.R., Wieringa J. (2000) Estimating the roughness of cities and sheltered country. Prepr. In: *12th AMS Conf. Applied Climatology* (Asheville, N.C.), 96-99.

De B. & Mukherjee M. (2014) Urban Physics for tomorrow's Urban Design. In *30th International PLEA Conference*, CEPT University, Ahmedabad.

Drexler J.Z., Snyder R.L., Spano D., Paw U.K.T. (2004) A review of models and micrometeorological methods used to estimate wetland evapotranspiration. *Hydrol Process* **18**(11), 2071-2101. doi: 10.1002/hyp.1462.

Efron B. & Tibshirani R. (1993) *An Introduction to the Bootstrap*. Chapman and Hall, New York.

Ellefsen R. (1991) Mapping and measuring buildings in the canopy boundary layer in ten U.S. cities. *Energy and Buildings* **16**(3-4), 1025-1049. doi: 10.1016/0378-7788(91)90097-M.

Fausto M.A., Machado N.G., Nogueira J.S., Biudes M.S. (2014) Net radiation estimated by remote sensing in Cerrado areas in the Upper Paraguay River Basin. *J Appl Remote Sens* **8**(1), 083541-1. doi: 10.1117/1.JRS.8.083541.

Grace J., Malhi Y., Lloyd J., Mcintyre J., Miranda A.C., Meir P., Miranda H.S. (1996). The use of eddy covariance to infer the net carbon diox-ide uptake of Brazilian rain forest. *Glob Change Biol* **2**, 209-217, doi: 10.1111/j.1365-2486.1996.tb00073.x.

Grimmond C.S.B., Cleugh H.A., Oke T.R. (1991) An objective heat storage model and its comparison with other schemes. *Atmos Environ* **25B**, 311-326, doi: 10.1016/0957-1272(91)90003-W.

Hu S., Zhao C., Li J., Wang F., Chen Y. (2013) Discussion and reassessment of the method used for accepting or rejecting data observed by a Bowen ratio system. *Hydrol Process* **28**, 4506–4510, doi: 10.1002/hyp.9962.

Li W., Fu R., Dickinson R.E. (2006) Rainfall and its seasonality over the Amazon. In: The 21st century as assessed by the coupled models for the IPCC AR4. *J Geophys Res*, 111, D0211, doi: 10.1029/2005JD006355.

Li Z., Barker H., Moreau L. (1995) The variable effect of clouds on atmospheric absorption of solar radiation. *Nature* **376**, 486-490, doi: 10.1038/376486a0.

Machado N.G., Biudes M.S., Angelini L.P., Mützenberg D.M.S., Nassarden D.C.S., Bilio R.S., Silva T.J.A., Neves G.A.R., Arruda P.H.Z., Nogueira J.S. (2016) Sazonalidade do Balanço de Energia e Evapotranspiração em Área Arbustiva Alagável no Pantanal Mato-Grossense. *Rev bras meteorol* **31**, 82-91, doi: 10.1590/0102-778620140164.

Machado N.G., Biudes M.S., Querino C.A.S., Danelichen V.H.M., Velasque M.C.S. (2014) Seasonal and interannual pattern of meteorological variables in Cuiabá, Mato Grosso State, Brazil. *Revista Brasileira de Geofísica* **33**, 1-12. doi: 10.22564/rbgf.v33i3.748.

Meyn S. & Oke T.R. (2009). Heat Fluxes Through Roofs and Their Relevance to Estimates of Urban Heat Storage. *Energy and Building* **41**, 745-752, doi: 10.1016/j.enbuild.2009.02.005.

Newton T., Oke T.R., Grimmond C.S.B., Roth M. (2007) The suburban energy balance in Miami, Florida. *Geografiska Annaler* **89**, 331-347. Available: www.jstor.org/stable/4621524.

Núñez, M. & Oke, T.R. (1977) The energy balance of an urban canyon. J Appl Meteor **16**, 11-19, Doi: 10.1175/1520-0450(1977)016<0011:TEBOAU>2.0.CO;2.

Offerle B., Grimmond C.S.B., Fortuniak K., Pawlak W. (2006) Intraurban Differences of Surface Energy Fluxes in a Central European City. *Journal of Applied Meteorology and Climatology* **45**, 125-136, doi: 10.1175/JAM2319.1.

Offerle B., Jonsson P., Eliasson I., Grimmond C.S.B. (2005) Urban Modification of the Surface Energy Balance in the West African Sahel: Ouagadougou, Burkina Faso. *J Climate* **18**, 3983–3995, doi: 10.1175/JCLI3520.1.

Oke T.R. (1987) *Boundary Layer Climates.* Routledge, New York.

Oke T.R. (2006) Initial guidance to obtain representative meteorological observations at urban sites. *Instruments and Observing Methods Report no. 81 WMO/ TD-No. 1250.*

Ortega-Farias S.O., Cuenca R.H., Ek M. (1996) Daytime variation of sensible heat flux estimated by the bulk aerodynamic method over a grass canopy. *Agric For Meteorol*, **81** 131-143. doi: 10.1016/0168-1923(95)02278-3.

Perez P.J., Castellvi F., Rosell J.I., Ibañez, M. (1999) Assessment of reliability of Bowen ratio method for partitioning fluxes. *Agri. For Meteorol* **97**, 141-150, doi: 10.1016/S0168-1923(99)00080-5.

Roberts S.M., Oke T.R., Grimmond C.S.B., Voogt J.A. (2006) Comparison of Four Methods to Estimate Urban Heat Storage. *J Appl Meteor Climatol* **45**, 1766-1781, doi: 10.1175/JAM2432.1.

Rodrigues T.R., Vourlitis G.L., Lobo F.A., Oliveira R.G., Nogueira, J.S. (2014) Seasonal variation in energy balance and canopy conductance for a tropical savanna ecosystem of south central Mato Grosso, Brazil. *J Geophys Res Biogeosci* **119**, 1-13, doi: 10.1002/2013JG002472.

Roth M. (2007) Review of urban climate research in (sub)tropical regions. *Int J Climatol* **27**, 1859-1873, doi: 10.1002/joc.1591.

Sailor D.J. & Lu L. (2004) A top-down methodology for developing diurnal and seasonal anthropogenic heating profiles for urban areas. *Atmos Environ* **38**, 2737–2748, doi: 10.1016/j.atmosenv.2004.01.034

Sun T., Wang Z.H., Oechel W.C., Grimmond C.S.B. (2017) The Analytical Objective Hysteresis Model (AnOHM v1.0): methodology to determine bulk storage heat flux coefficients, *Geosci Model Dev* **10**, 2875-2890. doi: 10.5194/gmd-10-2875-2017.

Unland H.E., Houser P.R., Shuttleworth W.J., Yang Z.L. (1996) Surface flux measurement and modelling at a semi-arid Sonoran Desert site. *Agric For Meteorol* **82**, 119–153, doi: 10.1016/0168-1923(96)02330-1.

Vourlitis G.L., Lobo F.A., Lawrence S., Lucena I.C., Borges Jr. O.B., Dalmagro H.J., Ortiz C.E.R.., Nogueira J.S. (2013) Variations in stand structure and diversity along a soil fertility gradient in a Brazilian savanna (Cerrado) in southern Mato Grosso. *Soil Sci Soc Am J* **77**, 1370-1379, doi: 10.2136/sssaj2012.0336.

Wang L.L., Gao Z.Q., Miao S.G., Guo X.F., Sun T., Liu M.F., Li D. (2015) Contrasting characteristics of the surface energy balance between the urban and rural areas of Beijing. *Adv Atmos Sci* **32**, 505-514, doi: 10.1007/s00376-014-3222-4.

Yoshida A., Tominaga K., Watatani S. (1991) Field measurements on energy balance of an urban canyon in the summer season. *Energy Building* **15**, 417–423, doi: 10.1016/0378-7788(90)90016-C.